PS/LEA/Note 86-5
4 juillet 1986

A Helix Coupler for a Pickup of a Low Velocity Beam

N.Tokuda[1)]

Abstract: A helix coupler of a travelling-wave type worked successfully as the pickup and the kicker in the stochastic momentum cooling of low velocity (β = 0.12) protons and α-particles stored in TARN (Test Accumulation Ring for Numatron) at INS, University of Tokyo. This coupler has a high coupling impedance and a bandwidth of a few hundred mega-hertz for such a low velocity beam. The presented formulation, based on the sheath helix model, explains well the measured coupling impedance at TARN, and is useful for optimization of the coupler's geometry to meet the required conditions: coupling impedance, bandwidth, and beam velocity.

---

1) On leave from the Institute for Nuclear Study, the University of Tokyo, Tokyo, Japan.

1. Introduction

Several types of couplers for pickups and kickers used in stochastic cooling have been considered to meet requirements on coupling impedance, bandwidth, beam velocity. The technique of stochastic cooling, which was originally developed to cool high−energy antiprotons, is now applied also to low−energy beams, for instance, the LEAR ring at CERN [1] (300 or 600 MeV/c antiprotons) and the TARN ring at INS [2] (115 MeV/c/nucleon protons and α−particles). It is an important subject to extend the beam velocity region to lower ranges, and many types of couplers should be examined to find an excellent coupler for a low−energy beam. As a candidate for such a coupler, a helix coupler of travelling wave type is presented here. This coupler was designed for momentum cooling at TARN, and worked successfully.

This paper describes the helix coupler used in the stochastic cooling at TARN, and its formulation based on the sheath helix model to calculate its coupling impedance and characteristic impedance.

2. Helix Coupler at TARN

Figure 1 shows the structure of the helix coupler used at TARN, and Table 1 lists its main parameters. The material is stainless steel. The helix and the shield are rectangles in the transverse cross section, because the profile of the rf−stacked beam is flat. The helix of 11.5 turns is wound around the four rods bolted to the two disks, which support the whole assembly in the vacuum chamber. The helix is insulated from the rods with dices of MACOOR. The shield is bolted to the two disks through L−metals.

The pitch of the helix is determined so that the signal's phase velocity in the longitudinal direction is equal to the beam velocity with an assumption that the signal propagates along the tape at the velocity of light. The reason for this determination of the pitch will become clear later, though the actual phase velocity is higher than the light velocity. As the characteristic impedance of the coupler measures 100 Ω, a 100 Ω transmission line, which is a two−conductor line with ceramic beads for insula-

tion, connects each output of the coupler to a feedthrough attached to the vacuum chamber. In the atmosphere, one of the feedthroughs is attached with a 100 Ω resistor for termination, and the other with a 100Ω/50Ω transformer for impedance matching between the coupler and the feedback system.

The measured coupling impedance derived from observed Schottky signal power of circulating particles is around 400 Ω in a frequency range from 50 to 100 MHz. The data will be shown later in Fig. 8 in comparison with theoretical values.

3. Formular for Coupling Impedance

The coupling impedance, or the sensitivity, of a pickup is defined by a ratio of output voltage from the pickup to the Fourier component of the beam current. As described by several authors [3, 4], the Lorentz's reciprocity theorem [5] enables us to obtain the output voltage of the pickup excited by the beam, whose position is (r_o,θ_o) in cylindrical coordinates, by calculating the longitudinal electric field component $E_z(r_o,\theta_o)$ and the power flow P_T through a coupler that is excited by a virtual external current source. In this paper, we consider a coupler of cylindrical structure and let the beam pass on the coupler's axis for simplicity of calculation. Then, in the context of Boussard and Di Massa [4], the coupling impedance is given by

$$Z_p = \frac{1}{2}\sqrt{\frac{R_o}{2P_T}}\, E_z(0)\, L\, |F(\xi)| \ , \tag{3.1}$$

$$F(\xi) \equiv \frac{\sin\xi}{\xi} \ , \tag{3.2}$$

$$\xi \equiv \frac{1}{2} k_o L \left(\frac{1}{\beta_b} - \frac{1}{\beta_w}\right) , \tag{3.3}$$

$$k_o \equiv \frac{\omega}{c} \ . \tag{3.4}$$

where L is the coupler length, R_o the load resistance, β_b the relative beam velocity, β_w the relative phase velocity of the signal, and k_o the propagation constant in free space. It should be noted that Eq.(3.1) is derived by assuming the load resistance R_o is equal to the characteristic impedance Z_c of the coupler. As will be described later, Z_c of a helix coupler varies with frequency; strictly speaking,

Eq.(3.1) is not accurate in our case. However, we use this equation, because it will be approximately correct, when the variation of Z_c is not large.

Our task here is to calculate phase velocity β_w and power flow P_T for a helix coupler. For the calculations to examine the properties of the TARN pickup, which as a rectangular cross section, we transform the pickup's geometry to a cylindrical one, whose circumference is equal to that of a rectangle. Then the parameters of the TARN pickup to be used in the calculation are summarized as in Table 2.

4. Sheath Helix Model

We consider a sheath helix, which approximates a tape helix, to simplify our problem. The sheath helix is a mechanically smooth metal pipe; however, the conductivity in the direction along the tape is infinite, whereas that in the direction perpendicular to the tape is zero (see Fig. 2). We have the following boundary conditions on the helix (r = a) and on the shield (r = b):

1) along the tape, the tangential electric field must vanish:

$$E_{\theta 1}\cos\psi + E_{z1}\sin\psi = 0 \quad , \tag{4.1}$$

$$E_{\theta 2}\cos\psi + E_{z2}\sin\psi = 0 \quad , \tag{4.2}$$

where the subscripts 1 and 2 refer to the field components in the two regions $0 \le r \le a$ and $a \le r \le b$;

2) the normal electric field must be continuous:

$$E_{z1}\cos\psi - E_{\theta 1}\sin\psi = E_{z2}\cos\psi - E_{\theta 2}\sin\psi \; ; \tag{4.3}$$

3) the tangential magnetic field must be continuous:

$$H_{z1}\sin\psi + H_{\theta 1}\cos\psi = H_{z2}\sin\psi + H_{\theta 2}\cos\psi \; ; \tag{4.4}$$

4) on the shield, the tangential electric fields must vanish:

$$E_{z2} = 0 \quad , \tag{4.5}$$

$$E_{\theta 2} = 0 \quad . \tag{4.6}$$

The electric field components are expressed in the form of a linear combination of modified Bessel functions with unknown constants A through F. With omission of the phase factor $e^{j(\omega t - kz)}$, they are

1) Region 1 ($0 \le r \le a$)

$$E_{z1} = A I_0(\gamma_0 r) , \tag{4.7}$$

$$E_{r1} = \frac{ik}{\gamma_0} A I_1(\gamma_0 r) , \tag{4.8}$$

$$H_{\theta 1} = \frac{1}{Z_0} E_{r1} . \tag{4.9}$$

$$H_{z1} = B I_0(\gamma_0 r) , \tag{4.10}$$

$$H_{r1} = \frac{ik}{\gamma_0} B I_1(\gamma_0 r) , \tag{4.11}$$

$$E_{\theta 1} = - Z_0 H_{r1} , \tag{4.12}$$

2) Region 2 ($a \le r \le b$)

$$E_{z2} = C I_0(\gamma_0 r) + D K_0(\gamma_0 r) , \tag{4.13}$$

$$E_{r2} = \frac{ik}{\gamma_0} [C I_1(\gamma_0 r) - D K_1(\gamma_0 r)] , \tag{4.14}$$

$$H_{\theta 2} = \frac{1}{Z_0} E_{r2} , \tag{4.15}$$

$$H_{z2} = E I_0(\gamma_0 r) + F K_0(\gamma_0 r) . \tag{4.16}$$

$$H_{r2} = \frac{ik}{\gamma_0} [E I_1(\gamma_0 r) - F K_1(\gamma_0 r)] , \tag{4.17}$$

$$E_{\theta 2} = - Z_0 H_{r2} , \tag{4.18}$$

where Z_0 is the impedance of vacuum ($120\pi\ \Omega$), and

$$\gamma_0 = k_0 \sqrt{\frac{1}{\beta_w^2} - 1} . \tag{4.19}$$

We have six unknown constants and six homogeneous equations derived from the boundary conditions of Eq.(4.1) through (4.6). To have a non-trivial solution for the unknown constants, the determinant must vanish. A straightforward calculation leads to

$$\frac{\tan\phi}{\tan\psi} = \frac{I_0(\gamma_0 a)}{I_1(\gamma_0 a)} \left[\frac{\frac{K_0(\gamma_0 a)}{I_0(\gamma_0 a)} - \frac{K_0(\gamma_0 b)}{I_0(\gamma_0 b)}}{\frac{K_1(\gamma_0 a)}{I_1(\gamma_0 a)} - \frac{K_1(\gamma_0 b)}{I_1(\gamma_0 b)}} \right]^{1/2} , \tag{4.20}$$

where the angle ϕ is defined by

$$\sin\phi \equiv \beta_w . \tag{4.21}$$

The transcendental equation provides the dispersion relation: the relation between phase velocity and frequency. Multiplying both sides of this equation by γ_0, we have another equation, whose left hand side is proportional to frequency:

$$k_0 a \cot\psi = \gamma_0 a \frac{I_0(\gamma_0 a)}{I_1(\gamma_0 a)} \left[\frac{\frac{K_0(\gamma_0 a)}{I_0(\gamma_0 a)} - \frac{K_0(\gamma_0 b)}{I_0(\gamma_0 b)}}{\frac{K_1(\gamma_0 a)}{I_1(\gamma_0 a)} - \frac{K_1(\gamma_0 b)}{I_1(\gamma_0 b)}} \right]^{1/2} . \qquad (4.22)$$

To obtain a solution of β_w for a given value of frequency and geometrical parameters, we should solve Eq.(4.22) numerically to compute γ_0 that satisfies this equation; it is straightforward to obtain β_w from the value of γ_0. The relation between $\tan\phi/\tan\psi$ and $k_0 a \cot\psi$ can be plotted on a graph as in Fig. 2, where curves for various values of b/a are shown. At the limit of f = 0,

$$\frac{\tan\phi}{\tan\psi} = \left[\frac{2\ln(b/a)}{1-(a/b)^2} \right]^{1/2} , \qquad (4.23)$$

or

$$\beta_w(0) = \left[\frac{2\ln(b/a)}{1-(a/b)^2 + 2\ln(b/a)\tan^2\psi} \right]^{1/2} \tan\psi , \qquad (4.24)$$

On the other hand, at high frequencies

$$\frac{\tan\phi}{\tan\psi} \sim 1 + \left(\frac{\tan\psi}{2k_0 a} \right)^2 , \qquad (4.25)$$

and in result

$$\beta_w \sim \left[1 + \left(\frac{\sin\psi}{2k_0 a} \right)^2 \right] \sin\psi . \qquad (4.26)$$

As is apparent in Fig. 3, phase velocity varies with frequency appreciably in the low−frequency region, especially for a large value of b/a, and decreases to c $\sin\psi$ asymptotically in the high frequency region.

The boundary conditions lead to electromagnetic fields are as follows.

$$E_{z1} = E_z(0) I_0(\gamma_0 r) , \qquad (4.27)$$

$$E_{r1} = \frac{j}{\cos\phi} E_z(0) I_1(\gamma_0 r) , \qquad (4.28)$$

$$E_{\theta 1} = -j Z_0 \tan\phi \, H_z(0) I_1(\gamma_0 r) , \qquad (4.29)$$

$$H_{z1} = H_z(0) I_0(\gamma_0 r) , \qquad (4.30)$$

$$H_{r1} = \frac{j}{\cos\phi} H_z(0) I_1(\gamma_0 r) , \qquad (4.31)$$

$$H_{\theta 1} = \frac{j}{Z_0} \tan\phi \, E_z(0) \, I_1(\gamma_0 r) , \qquad (4.32)$$

$$E_{z2} = E_z(0) \frac{T_0(\gamma_0 b) - T_0(\gamma_0 r)}{T_0(\gamma_0 b) - T_0(\gamma_0 a)} I_0(\gamma_0 r) , \qquad (4.33)$$

$$E_{r2} = \frac{j}{\cos\phi} E_z(0) \frac{T_0(\gamma_0 b) + T_1(\gamma_0 r)}{T_0(\gamma_0 b) - T_0(\gamma_0 a)} I_1(\gamma_0 r) , \qquad (4.34)$$

$$E_{\theta 2} = -j Z_0 \tan\phi \, H_z(0) \frac{T_1(\gamma_0 b) - T_1(\gamma_0 r)}{T_1(\gamma_0 b) - T_1(\gamma_0 r)} I_1(\gamma_0 r) , \qquad (4.35)$$

$$H_{z2} = H_z(0) \frac{T_1(\gamma_0 b) + T_0(\gamma_0 r)}{T_1(\gamma_0 b) - T_1(\gamma_0 a)} I_0(\gamma_0 r) , \qquad (4.36)$$

$$H_{r2} = \frac{j}{\cos\phi} H_z(0) \frac{T_1(\gamma_0 b) - T_1(\gamma_0 r)}{T_1(\gamma_0 b) - T_1(\gamma_0 r)} I_1(\gamma_0 r) , \qquad (4.37)$$

$$H_{\theta 2} = \frac{j}{Z_0} \tan\phi \, E_z(0) \frac{T_0(\gamma_0 b) + T_1(\gamma_0 r)}{T_0(\gamma_0 b) - T_0(\gamma_0 a)} I_1(\gamma_0 r) , \qquad (4.38)$$

where

$$T_i(x) \equiv \frac{K_i(x)}{I_i(x)} \quad (i = 0, 1) , \qquad (4.39)$$

$$H_z(0) = -\frac{j}{Z_0} \frac{\tan\psi}{\tan\phi} \frac{I_0(\gamma_0 a)}{I_1(\gamma_0 a)} E_z(0) . \qquad (4.40)$$

5. Synchronism of phase velocity and beam velocity

From the dispersion relation, we obtain phase velocity as a function of frequency, and can examine the behavior of the factor F(ξ) defined by Eq.(3.2). At f = 0, the parameterr ξ vanishes, and conseq-uently F(ξ) = 1. At f = ∞,

$$\lim_{f \to \infty} F(\xi) = \begin{cases} 1 & (\sin\psi = \beta_b) \\ 0 & (\sin\psi \neq \beta_b) \end{cases} , \qquad (5.1)$$

as is derived from Eq.(4.26). Therefore, the pitch angle should be set so that $\sin\psi = \beta_b$, or the coupling impedance is reduced at high frequencies due to the damping of F(ξ). Figure 4 shows F(ξ) as a function of frequency for various values of $\beta_b/\sin\psi$; the geometry of the coupler is that of the TARN pickup. This figure indicates that the applicable beam−velocity region is wide, when the required bandwidth is narrow. For instance, when the required upper limit of the bandwidth is 100 MHz, F(ξ)

exceeds 0.5 in a velocity region from β_b = 0.1 to 0.2, as shown in Fig. 5. It should be noted that the length is an important parameter in F(ξ). At a long coupler, F(ξ) decreases at high frequencies; therefore, a long coupler does not mean a high coupling impedance, though Eq.(3.1) seems to say that coupling impedance is proportional to length. The relation between coupling impedance and length will be discussed in Sect. 9.2 in more detail.

6. Power Flow

The power flow through the coupler is obtained by calculating the Poynting vector

$$P_T = \frac{1}{2} Re \iint (\vec{E} \times \vec{H}^*) \cdot \vec{n}_z \, dS$$
$$= \pi Re \int_0^b (E_r H_\theta^* - E_\theta H_r^*) \, r \, dr \, . \qquad (6.1)$$

Putting the electromagnetic fields obtained in Sect. 4, we have

$$P_{T1} = \frac{\pi}{2} \frac{|E_z(0)|^2}{Z_0} a^2 \frac{\tan^2\psi}{\beta_w} \frac{I_0^2(\gamma_0 a)}{I_1^2(\gamma_0 a)} \left[1 + \frac{T_0(\gamma_0 a) - T_0(\gamma_0 b)}{T_1(\gamma_0 a) - T_1(\gamma_0 b)} \right]$$
$$\times \left[I_1^2(\gamma_0 a) - I_0(\gamma_0 a) I_2(\gamma_0 a) \right] \qquad (6.2)$$

for the inside of the helix, and

$$P_{T2} = \frac{\pi}{2} \frac{|E_z(0)|^2}{Z_0} \frac{1}{\gamma_0^2} \frac{\tan^2\psi}{\beta_w} \frac{I_0^2(\gamma_0 a)}{I_1^2(\gamma_0 a)} \frac{1}{T_1(\gamma_0 a) - T_1(\gamma_0 b)}$$
$$\times \left\{ - \frac{\frac{1}{I_0^2(\gamma_0 a)} - \frac{1}{I_0^2(\gamma_0 b)}}{T_0(\gamma_0 a) - T_0(\gamma_0 b)} + \frac{\frac{1}{I_1^2(\gamma_0 a)} - \frac{1}{I_1^2(\gamma_0 b)}}{T_1(\gamma_0 a) - T_1(\gamma_0 b)} \right.$$
$$+ (\gamma_0 a)^2 \left[I_1^2(\gamma_0 a) - I_0(\gamma_0 a) I_2(\gamma_0 a) \right]$$
$$\left. \times \left[T_0(\gamma_0 a) + T_1(\gamma_0 a) + T_0(\gamma_0 b) + T_1(\gamma_0 b) \right] \right\} \qquad (6.3)$$

for the outside of the helix. The sum of them is

$$P_T = \frac{\pi}{2} \frac{|E_z(0)|^2}{Z_0} \frac{1}{k_0^2} \frac{\beta_w^3}{(1-\beta_w^2)^2} \frac{1}{T_0(\gamma_0 a) - T_0(\gamma_0 b)}$$
$$\times \left\{ 4 + 2\gamma_0 a \left(\frac{I_1(\gamma_0 a)}{I_0(\gamma_0 a)} - \frac{I_0(\gamma_0 a)}{I_1(\gamma_0 a)} \right) \right.$$
$$\left. - \frac{\frac{1}{I_0^2(\gamma_0 a)} - \frac{1}{I_0^2(\gamma_0 b)}}{T_0(\gamma_0 a) - T_0(\gamma_0 b)} + \frac{\frac{1}{I_1^2(\gamma_0 a)} - \frac{1}{I_1^2(\gamma_0 b)}}{T_1(\gamma_0 a) - T_1(\gamma_0 b)} \right\} . \qquad (6.4)$$

In the calculation of the integral of the modified Bessel functions, the following formulae are used:

$$\int I_1^2(\gamma x)\, x\, dx = \frac{x^2}{2}\left[I_1^2(\gamma x) - I_0(\gamma x) I_2(\gamma x) \right] , \tag{6.5}$$

$$\int K_1^2(\gamma x)\, x\, dx = \frac{x^2}{2}\left[K_1^2(\gamma x) - K_0(\gamma x) K_2(\gamma x) \right] , \tag{6.6}$$

$$\int I_1(\gamma x) K_1(\gamma x)\, x\, dx = \frac{x^2}{2}\left[I_1(\gamma x) K_1(\gamma x) + \frac{1}{2} I_0(\gamma x) K_2(\gamma x) + \frac{1}{2} I_2(\gamma x) K_0(\gamma x) \right] . \tag{6.7}$$

We introduce normalized power flow, which is power flow divided by $|E_z(0)|^2$:

$$P_{Tn1} \equiv P_{T1} / |E_z(0)|^2 , \tag{6.8}$$

$$P_{Tn2} \equiv P_{T2} / |E_z(0)|^2 , \tag{6.9}$$

$$P_{Tn} \equiv P_T / |E_z(0)|^2 . \tag{6.10}$$

Their limiting values at f = 0 and f = ∞ are

$$\lim_{f \to 0} P_{Tn1} = \frac{\pi}{4 Z_0} a^2 \frac{\tan^2 \psi}{\beta_w(0)} , \tag{6.11}$$

$$\lim_{f \to \infty} P_{Tn1} = \infty , \tag{6.12}$$

$$\lim_{f \to 0, \infty} P_{Tn2} = \infty , \tag{6.13}$$

$$\lim_{f \to 0, \infty} P_{Tn} = \infty . \tag{6.14}$$

Therefore the coupling impedance, which is inversely proportional to the square root of P_{Tn}, vanishes at f = 0 and ∞, and takes a maximum value at a certain frequency; thus, the coupler has a finite bandwidth. Figure 6 shows the normalized power flow for the geometry of the helix pickup of TARN.

7. Characteristic Impedance

We define the characteristic impedance by

$$Z_c = \frac{|V|^2}{2 P_T} , \tag{7.1}$$

where V is the voltage between the helix and the shield:

$$V = -\int_a^b E_{r2}\, dr$$

$$= \frac{ik}{\gamma_0^2} I_0(\gamma_0 a) E_z(0) \quad . \tag{7.2}$$

Putting this equation into Eq.(7.1), we have

$$Z_c = \frac{1}{2k_0^2} \left(\frac{\beta_w}{1-\beta_w^2} \right)^2 I_0^2(\gamma_0 a)\, P_{Tm}^{-1} \quad . \tag{7.3}$$

At the limits of f = 0 and ∞,

$$\lim_{f \to 0} Z_c = \frac{Z_0}{2\pi} \frac{\ln(b/a)}{\beta_w(0)} \quad , \tag{7.4}$$

$$\lim_{f \to \infty} Z_c = 0 \quad . \tag{7.5}$$

Figure 7 shows Z_c as a function of frequency. For a large value of b/a, Z_c varies appreciably with frequency. Therefore, a small value of b/a is desirable from the view point of impedance matching between the coupler and the 50 Ω feedback system.

8. Coupling Impedance

The theoretical values of the coupling impedance for the geometry of the TARN pickup are shown in Fig. 8, where the experimental values are plotted in good agreement with the theoretical values. The solid line is the result with R_0 = 177 Ω, which is the theoretical characteristic impedance at 0 MHz given by Eq.(7.4); the dashed line is that with R_0 = 100 Ω, which is the measured one. The measured characteristic impedance is almost constant at this value in a frequency range up to 100 MHz. The reason for the discrepancy between the theoretical value and the experimental one has not been clarified. The experimental coupling impedance is derived from the measured Schottky signal power; the power per Schottky band is given by

$$P_S = 2(qe)^2 f_0^2 \frac{|Z_P|^2}{Z_c} \quad , \tag{8.1}$$

where q is the charge number of the ion, f_0 the revolution frequency, and Z_c = 100 Ω. The data of Schottky signals of 7 MeV/n protons and α − particles are used here.

9. Discussion on Parameter Setting

9.1 Pitch angle

Once the beam velocity is determined, the pitch angle should be automatically set so that $\sin\psi = \beta_b$. Though the Fig. 4 shows a value of $\sin\psi = \beta_b/1.1$ or $\beta_b/1.2$ porvides a slightly larger value of $|F(\xi)|$ at low frequencies than that of $\sin\psi = \beta_b$, $\sin\psi$ should be equal to β_b to attain a wider band-width.

The dependence of coupling impedance on pitch angle is shown in Fig. 9. For the case of $\sin\psi = 0.05$, the coupling impedance rises steeply with frequency and a large maximum value; therefore, the helix coupler suits a low−velocity beam. The large maximum value of Z_p is attributed to a large value of load resistance of 429 Ω, which is equal to the value of the characteristic impedance at 0 MHz. As is apparent in Fig. 10, characteristic impedance varies appreciably with frequency for a small value of pitch angle. Therefore, the mismatching of impedance will lead to smaller coupling impedance than the theoretical one.

9.2 Length

As mentioned in Sec. 5, coupling impedance is not proportional to length owing to the factor $F(\xi)$, which is a function of length. The length should be optimized not only from the point of view of high coupling impedance but that of applicable beam−velocity range; because, a short coupler gains a wide beam−velocity range at a cost of coupling impedance. Figure 11 shows coupling impedance as a function of frequency for length of 36.2, 72.4, 144.8, and 217.2 cm (0.5 : 1 : 2 : 3); the other geometrical parameters are as same as the TARN pickup. Up to the length of 144.8 cm, the coupling impedance increases with length, but the extention of the length to 217.2 cm does not effect a high coupling impedance. Figures 12 (a) and (b) show coupling impedances for beam velocities $\beta_b = 0.1$ and 0.2, respectively. The couplers of 36.2 and 72.4 cm might be applicable to these beams in a frequency range below ~ 150 MHz, but those of 144.8 and 217.2 cm are not. For a short coupler of 36.2 cm, coupling impedances at 50, 100, and 150 MHz are shown in Fig. 13 as a function of beam veloci-

ty. If the required bandwidth is narrower than 100 MHz, this coupler is applicable even to a relativistic beam.

9.3 Radiuses

The radius of the helix is determined by the beam size. So we have to optimize the shield radius or the ratio of b/a. Figure 14 shows coupling impedance as a funciton of frequency for various values of b/a. For a large value of b/a, coupling impedance takes a large value. This is caused by R_o set at a charactristic impedance at 0 MHz, which increases with b/a. We should note that a large b/a leads to appreciable variation of characteristic impedance with frequency, as discussed in Sec. 7. Therefore the value of b/a should be set at an approriate value from the point of view of impedance matching.

10. Conclusion

The coupling impedance of a helix coupler has been formulated. The calculated coupling impedance agrees well with the experimental data at TARN. The characteristics of the coupler have been examined for various coupler's geometries: ratio of shield radius to helix radius, pitch angle, and length. In result, a helix coupler turned out to provide a coupling impedance of several hundred ohms in a frequency range of a few hundred mega−hertzs; moreover, a short coupler gains a wide range of applicable beam velocity.

Acknowledgments

The cooling experiment at TARN was carried out under the leadership of T. Katayama by members of the Accelerator Research Division of INS. The author thanks them for their collaboration in various aspects through this experiment, and owes H. Yonehara and M. Yoshizawa the off-line analysis of the spectrum-analyzer data and the derivation of the coupling impedance data presented in this paper. The theoretical analysis described here was finished during the author's stay at the CERN LEAR Group; he express his sincere thanks to P. Lefèvre and D. Möhl, who gave him a chance to visit CERN and encouraged in this work. Thanks are also due to S. Baird, who edited the manuscript.

References

[1] The LEAR Team, "Performance of LEAR", The 1985 Particle Accelerator Conference, Vancouver, B.C., Canada, 1985: IEEE Trans. on Nucl. Sci., Vol.NS-32, No.5, 1985.

[2] N. Tokuda et al., "Stochastic Momentum Cooling of a Low Energy Beam at TARN", ibid.

[3] J. Bisognano and C. Leemann, "Stochastic Cooling", Proc. of Physics of High Energy Particle Accelerators, Fermilab Summer School, 1981: AIP Conference Proceedings No.87, 1982.

[4] D. Boussard and G. Di Massa, "High Frequency Slow Wave Pick-ups", CERN Report, CERN SPS/86-4 (ARF), 1986.

[5] R. E. Collin, "Foundations for Microwave Engineering", McGraw-Hill, 1966.

Table 1: Main parameters of the TARN pickup

Helix	
Cross section	19.7 cm × 5.7 cm
Tape width	1 cm
No. of turns	11.5
Pitch	6.1 cm
Shield	
Cross section	26.7 cm × 12.7 cm
Length	72.4 cm
Characteristic impedance (meas.)	~ 100Ω
Relative beam velocity	0.12147 (7 MeV)

Table 2: Parameters of the TARN pickup to be used in the calculations

Helix radius (a)	8.09 cm
Shield radius (b)	12.54 cm
Length (L)	72.4 cm
Pitch angle (ψ)	$\sin^{-1}0.12147$
Relative beam velocity (β_b)	0.12147 (7 MeV)

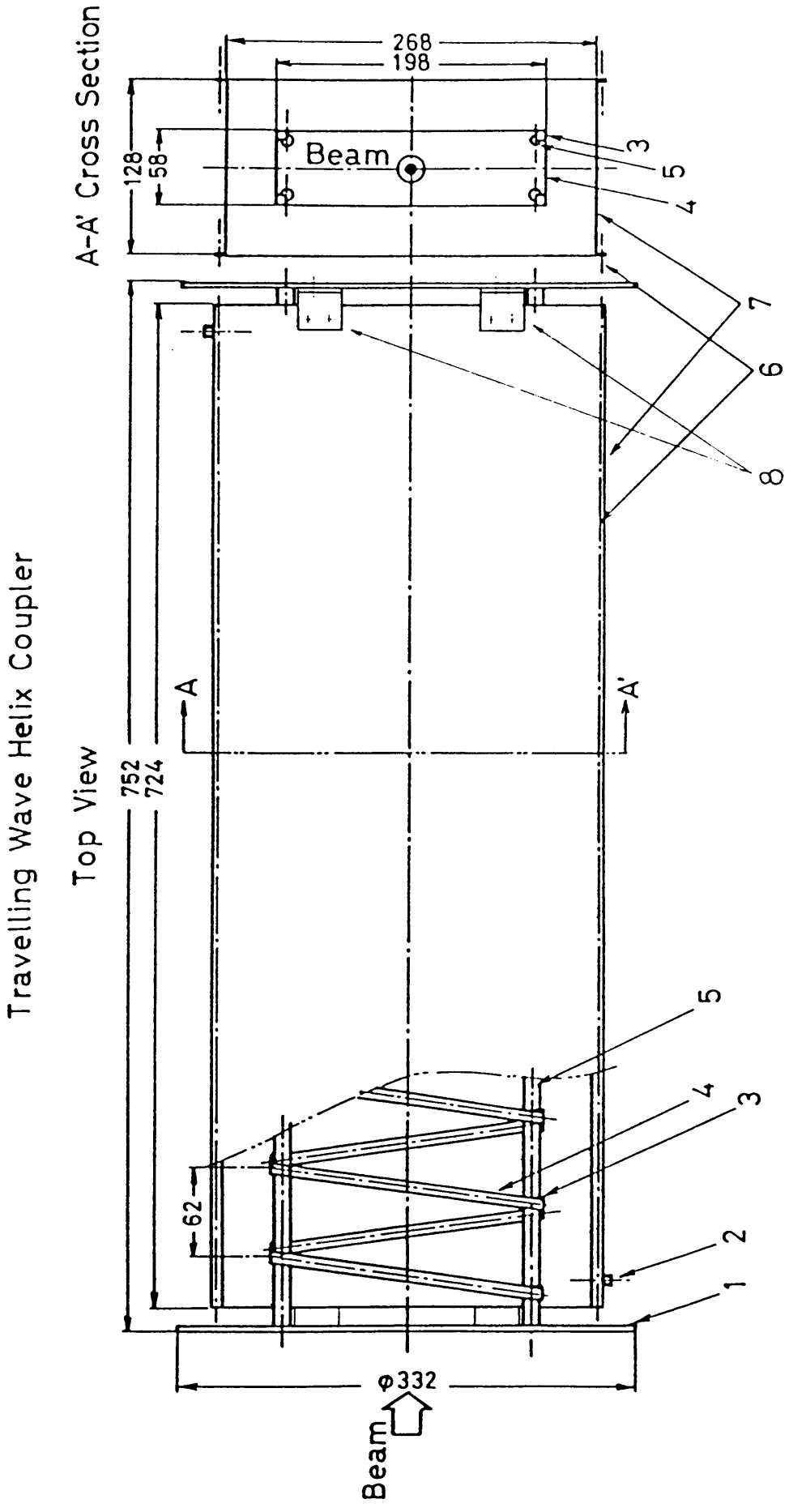

Fig. 1. The structure of the helix coupler used at TARN. The unit of length is mm. 1) disk for the support of the assembly, 2) feedthrough for the two – conductor transmission line, 3) MACOOR insulator between the helix and the rods, 4) 11.5 – turn helix tape of 0.1 mm in thickness and 10 mm in width, 5) rod for the support of the helix, 6) bolts to fasten the shield, 7) shield of 1 mm in thickness, 8) L – metal to fix the shield to the disks.

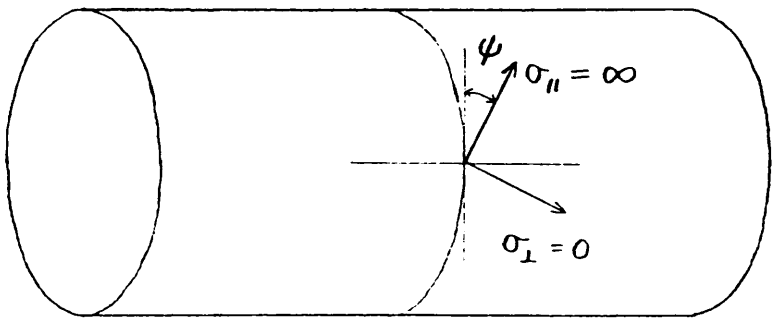

Fig. 2. A sheath helix, an approximation of a tape helix. The conductivity in the direction along the tape is infinite, whereas that in the direction perpendicular to the tape is zero.

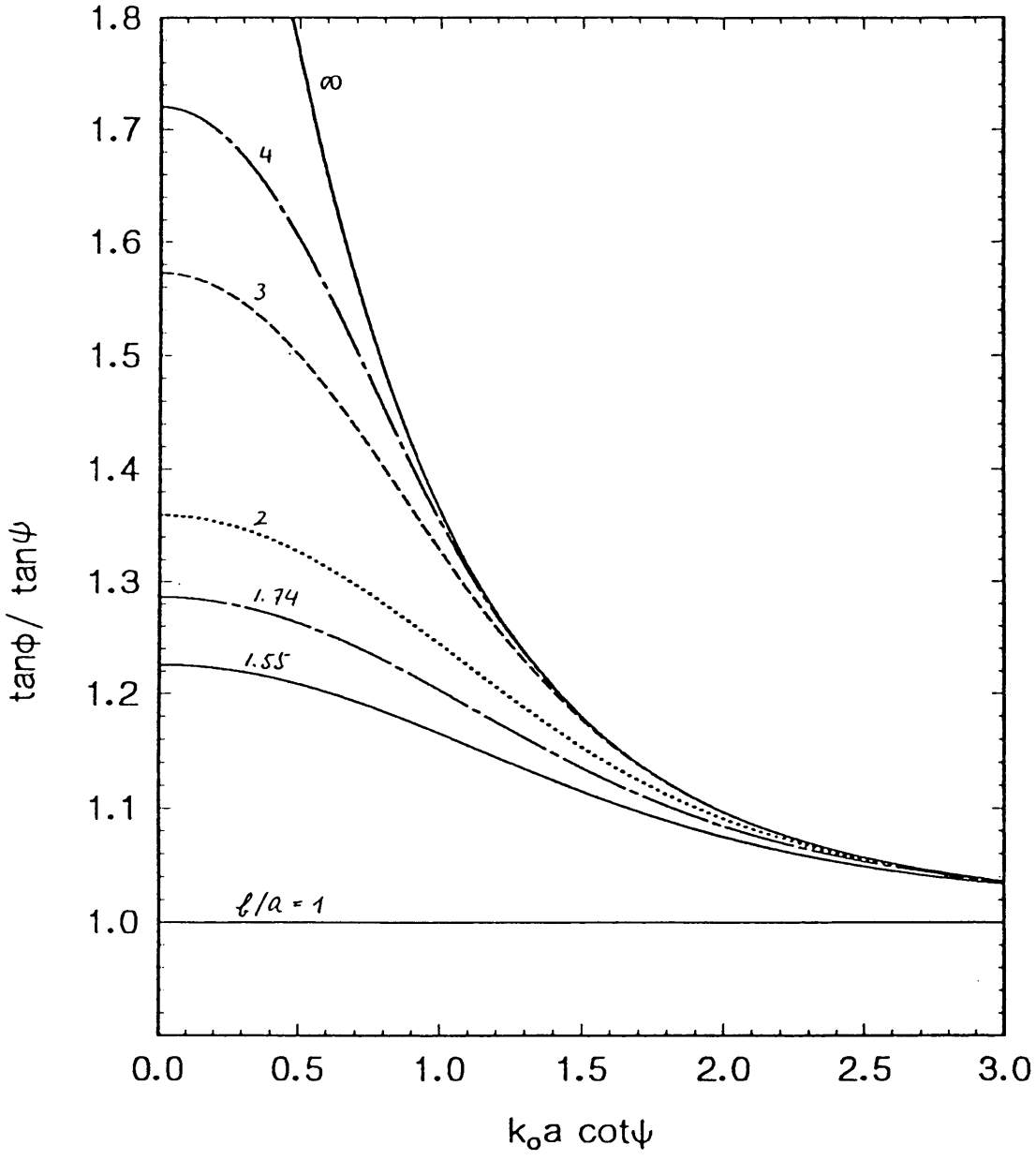

Fig. 3. Dispersion relation for various values of b/a. The ordinate means phase velocity, and the abscissa frequency. For the geometry of at TARN, b/a = 1.55 and, k_o a cotψ = 1.39 at 100 MHz.

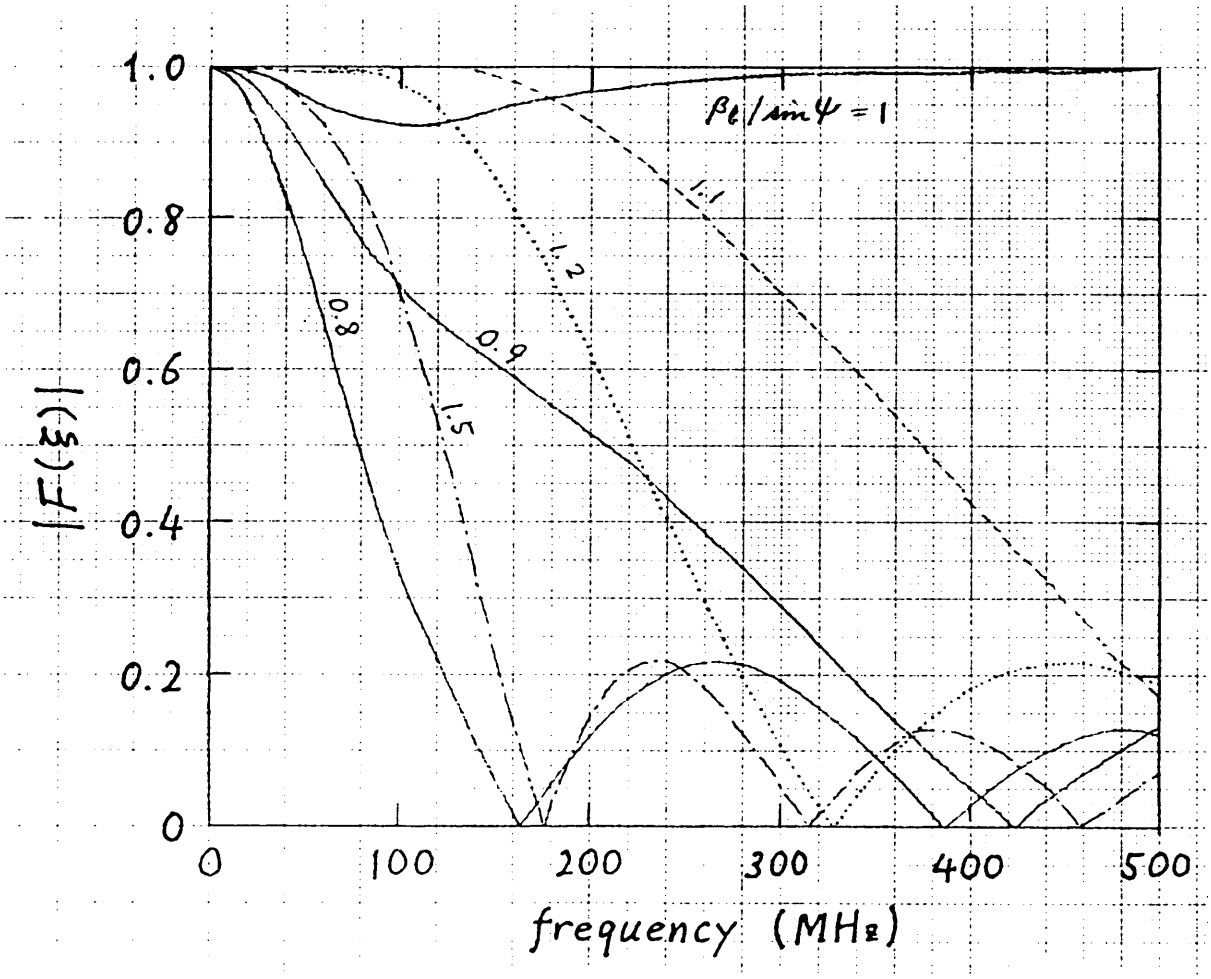

Fig. 4. Profile of $|F(\xi)|$ for various values of $\beta_b/\sin\psi$. The geometry of the coupler is that of the TARN pickup. The pitch angle should be set so that $\sin\psi = \beta_b$ to keep $|F(\xi)|$ as high as unity up to a high frequency region.

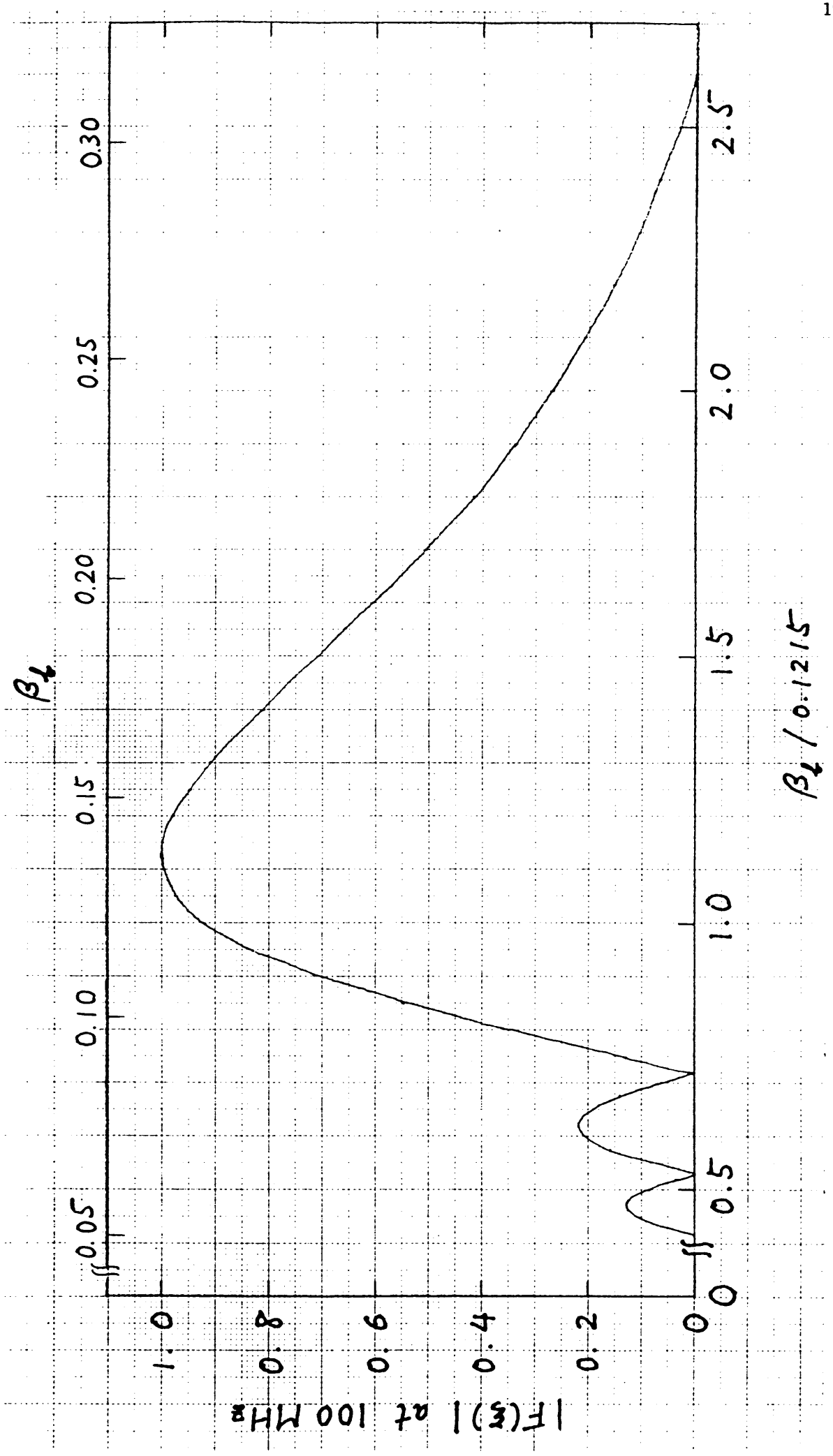

Fig. 5. |F(ξ)| at 100 MHz as a function of beam velocity. The geometry of the coupler is that of the TARN pickup. |F(ξ)| is larger than 0.5 in a beam – velocity region from β_b = 0.1 (T = 5 MeV, p = 96 MeV/c) to 0.2 (19 MeV, 192 MeV/c).

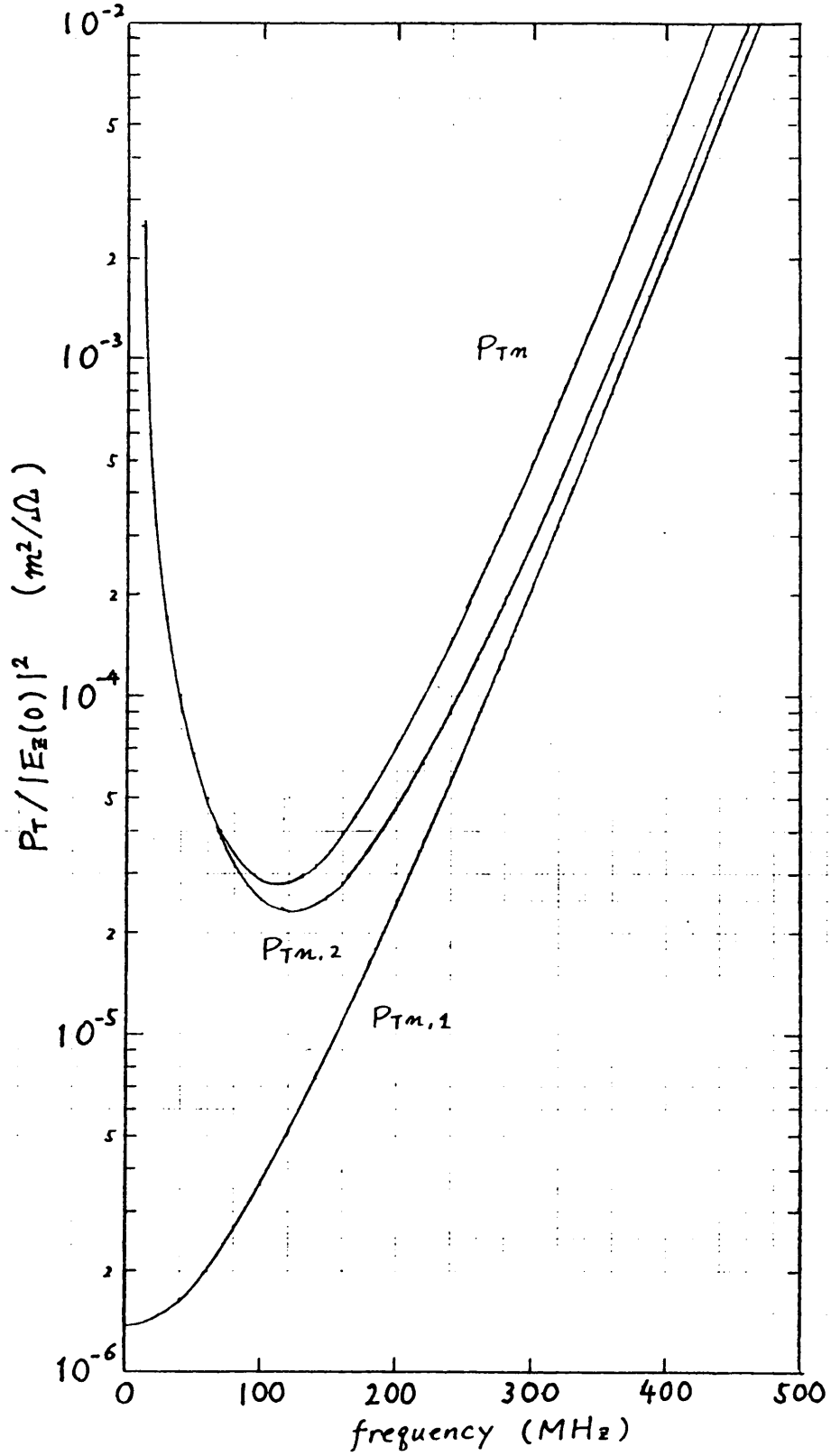

Fig. 6. Normalized power flow for the geometry of the TARN pickup.

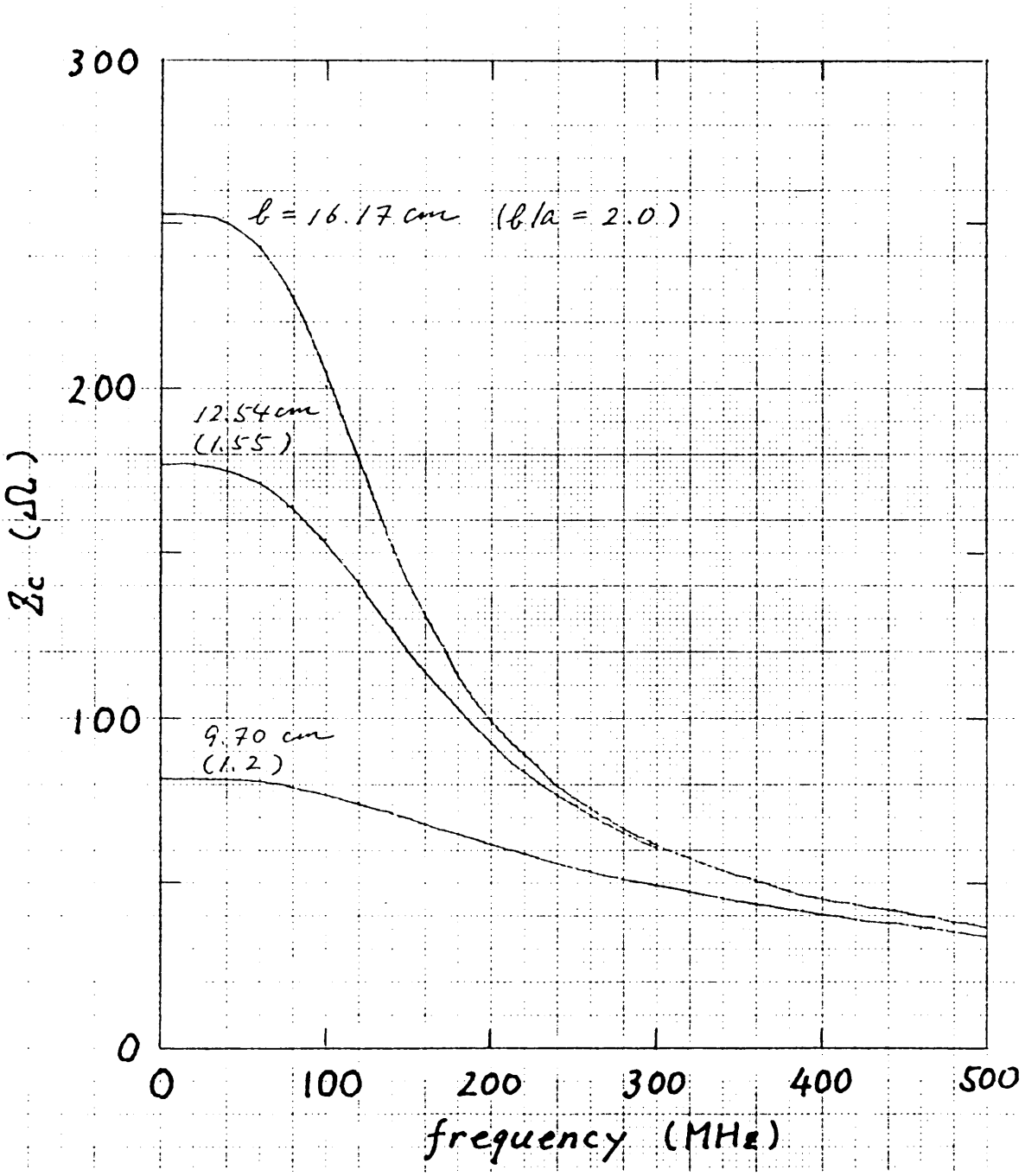

Fig. 7. Characteristic impedance for some values of shield radius: 9.70 cm (b/a = 1.2), 12.54 cm (1.55), and 16.17 cm (2.0). The helix radius is 8.09 cm, and $\sin\psi$ = 0.12147, same as the TARN pickup.

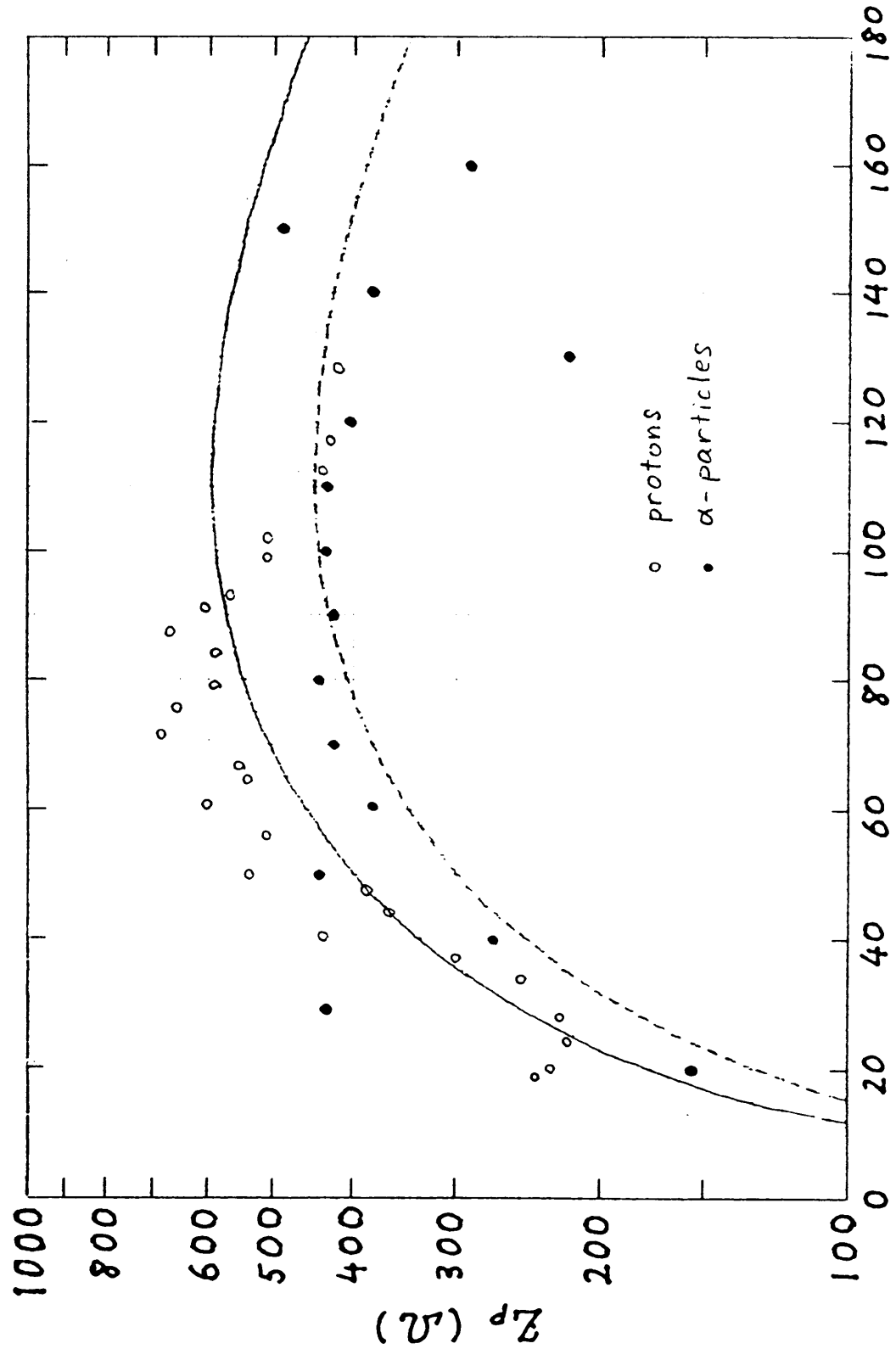

Fig. 8. Calculated coupling impedance in comparison with experimental data at TARN. The solid line is the theoretical result with R_Q = 177 Ω, equal to the theoretical characteristic impedance at 0 MHz, and the dashed line is that with R_o = 100 Ω, equal to the measured one.

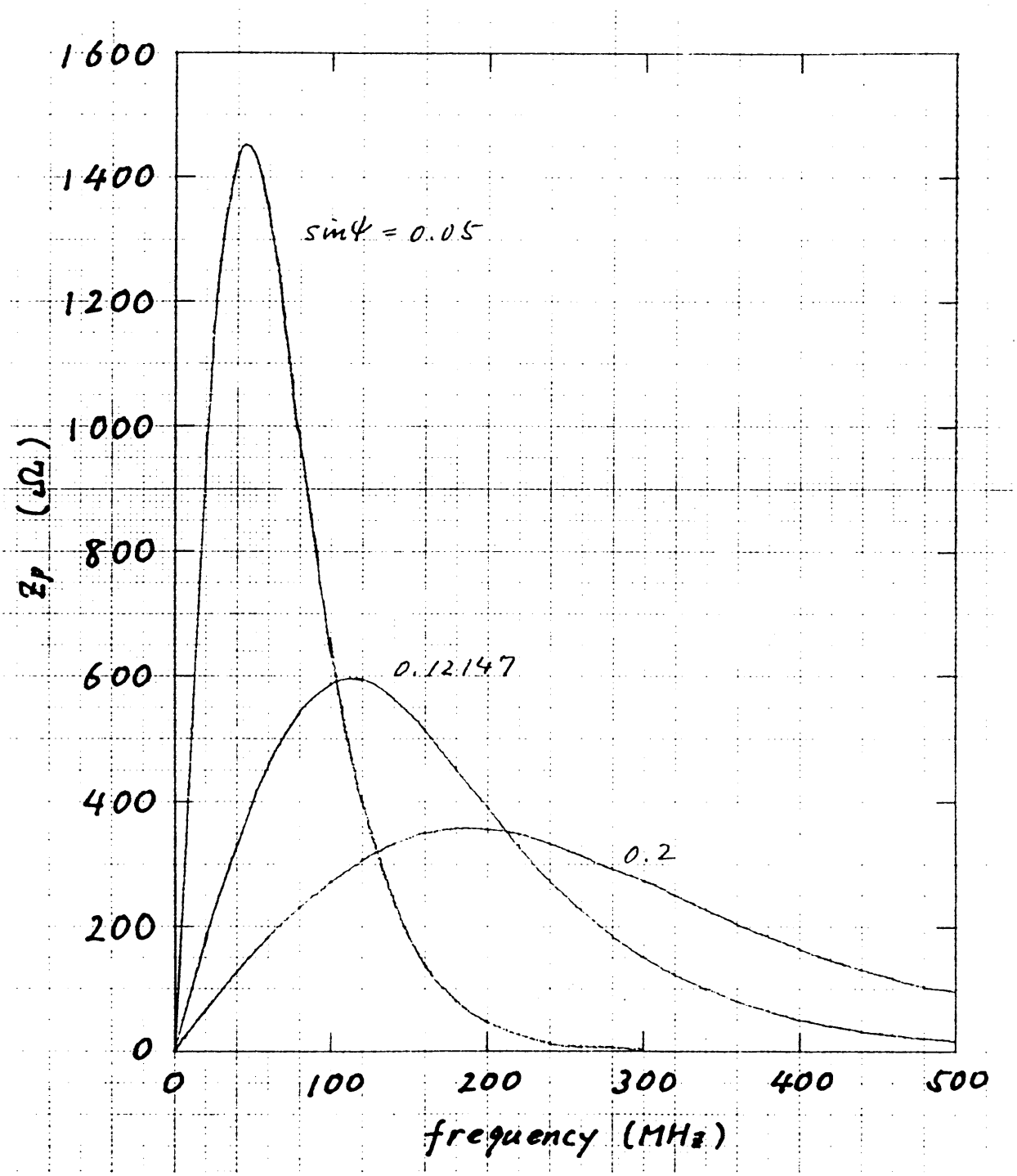

Fig. 9. Coupling impedance for some values of pitch angle. The other geometrical parameters are same as those of the TARN pickup, and $\beta_b = \sin\psi$. The load impedances are 429 Ω for $\sin\psi = 0.05$, 177 Ω for 0.12147, and 108 Ω for 0.2; they are equal to characteristics impedance at 0 MHz.

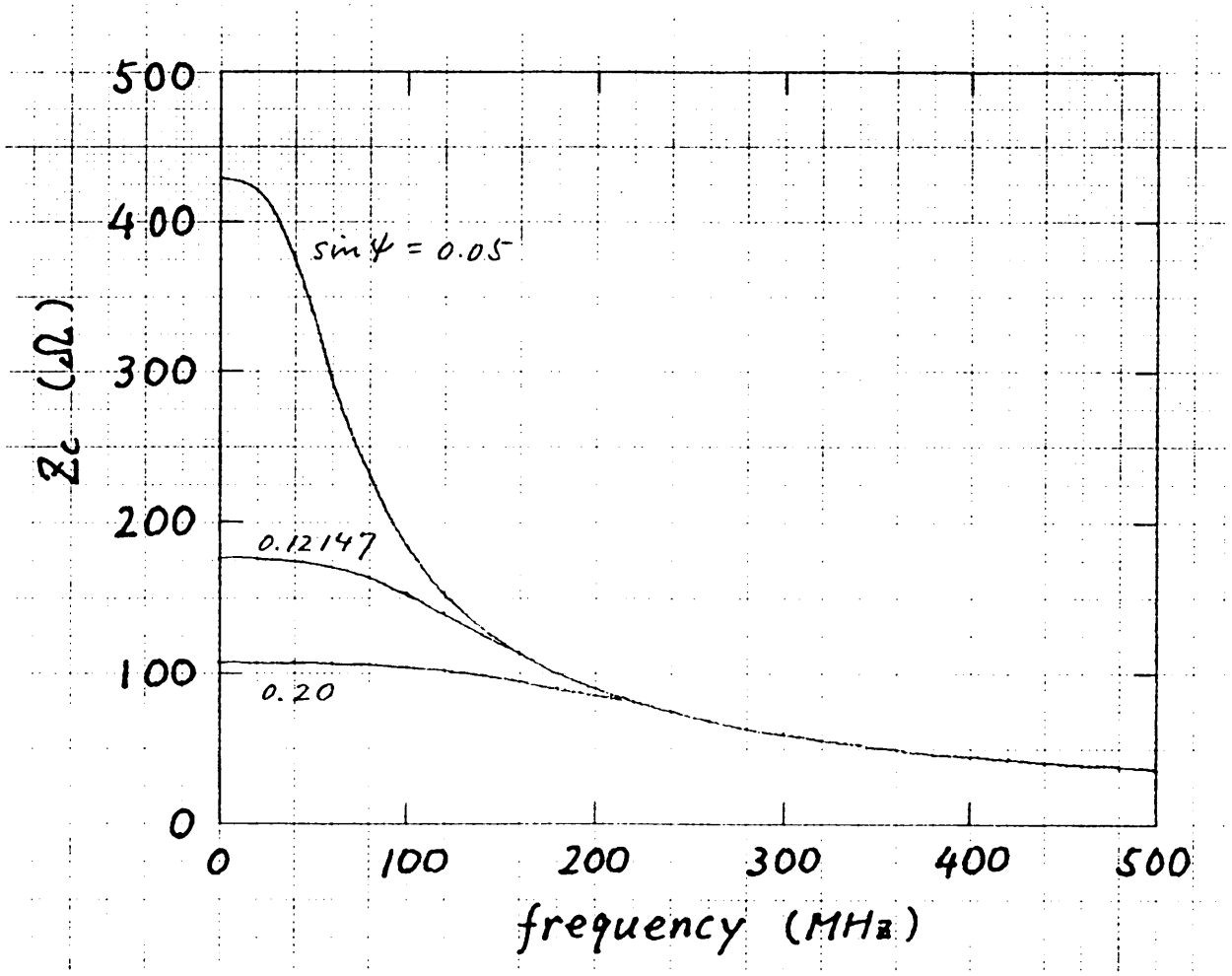

Fig. 10. Characteristic impedance for some values of pitch angle. The helix radius is 8.09 cm, and the shield radius is 12.54 cm.

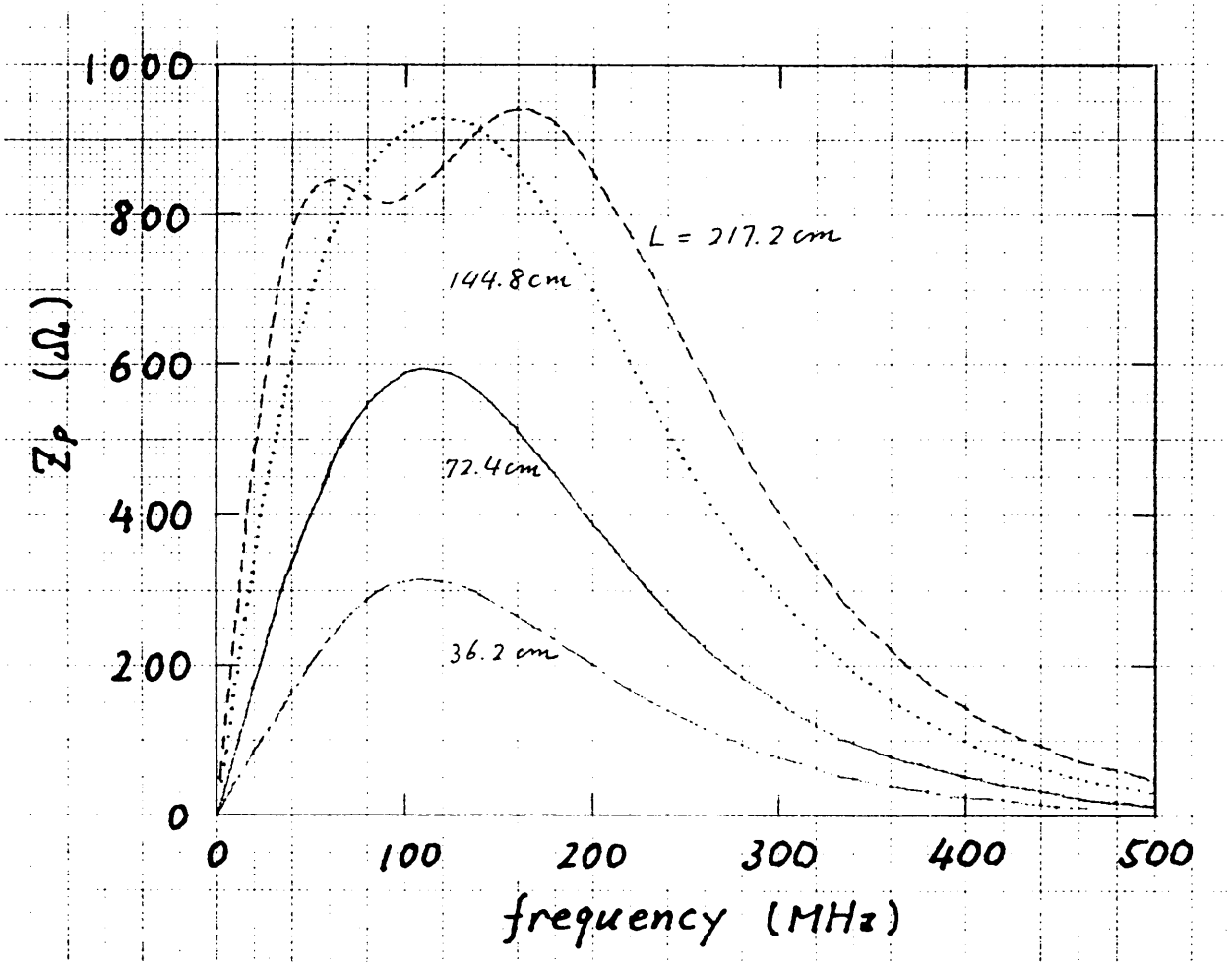

Fig. 11. Coupling impedance for various values of length: 36.2 cm (dash−dotted line), 72.4 cm (solid line), 144.8 cm (dotted line), and 217.2 cm (dashed line). The other geometrical parameters are same as the TARN pickup, and R_o = 177 Ω. The relative beam velocity is equal to sinψ.

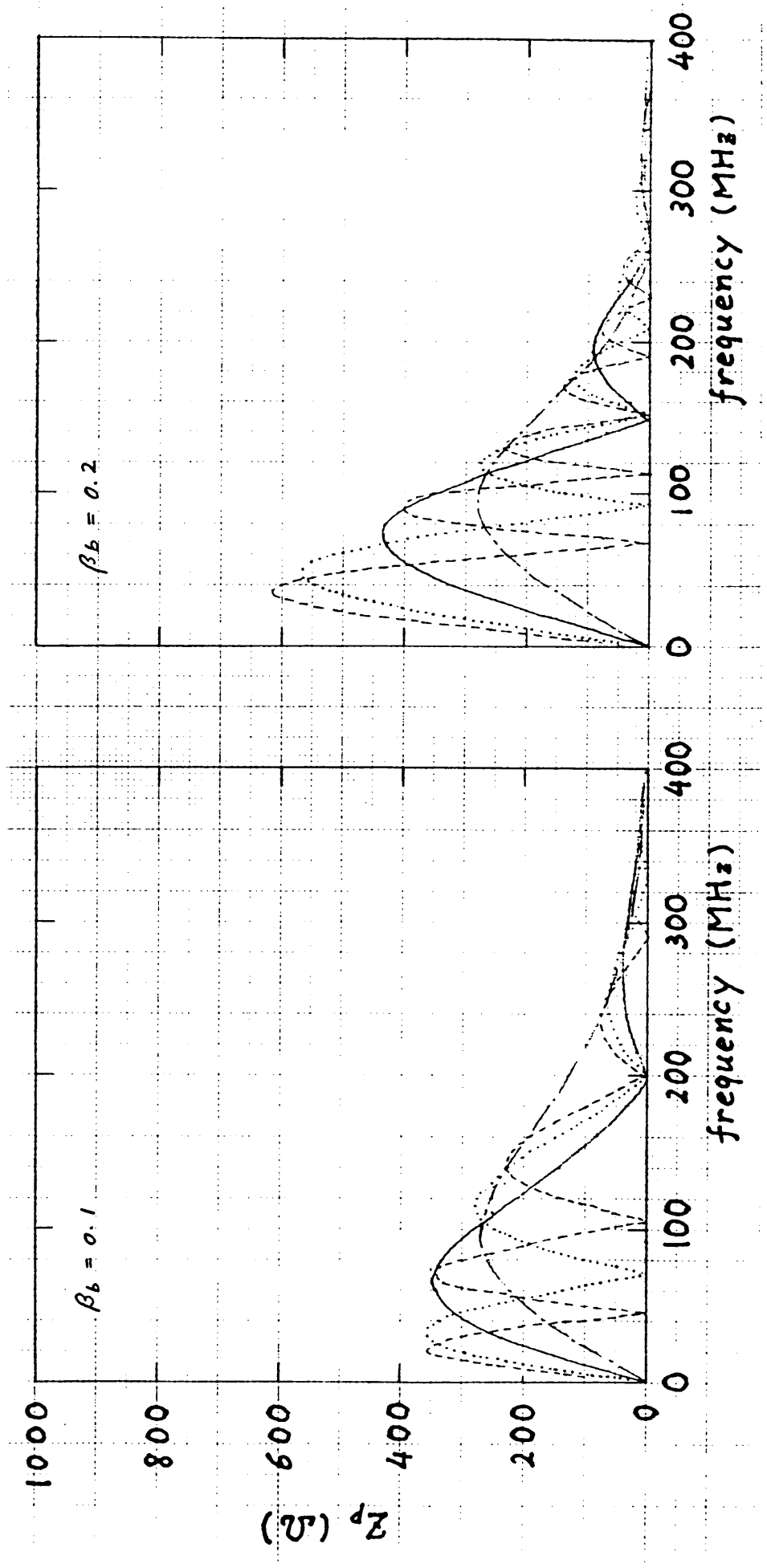

Fig. 12. Coupling impedance for relative beam velocities different from $\sin\psi = 0.12147$: $\beta_b = 0.1$ at Fig. 12(a), and 0.2 at Fig. 12(b). The four curves in each of the figures correspond to couplers of 36.2 cm (dash – dotted line), 72.4 cm (solid line), 144.8 cm (dotted line), and 217.2 cm (dashed line).

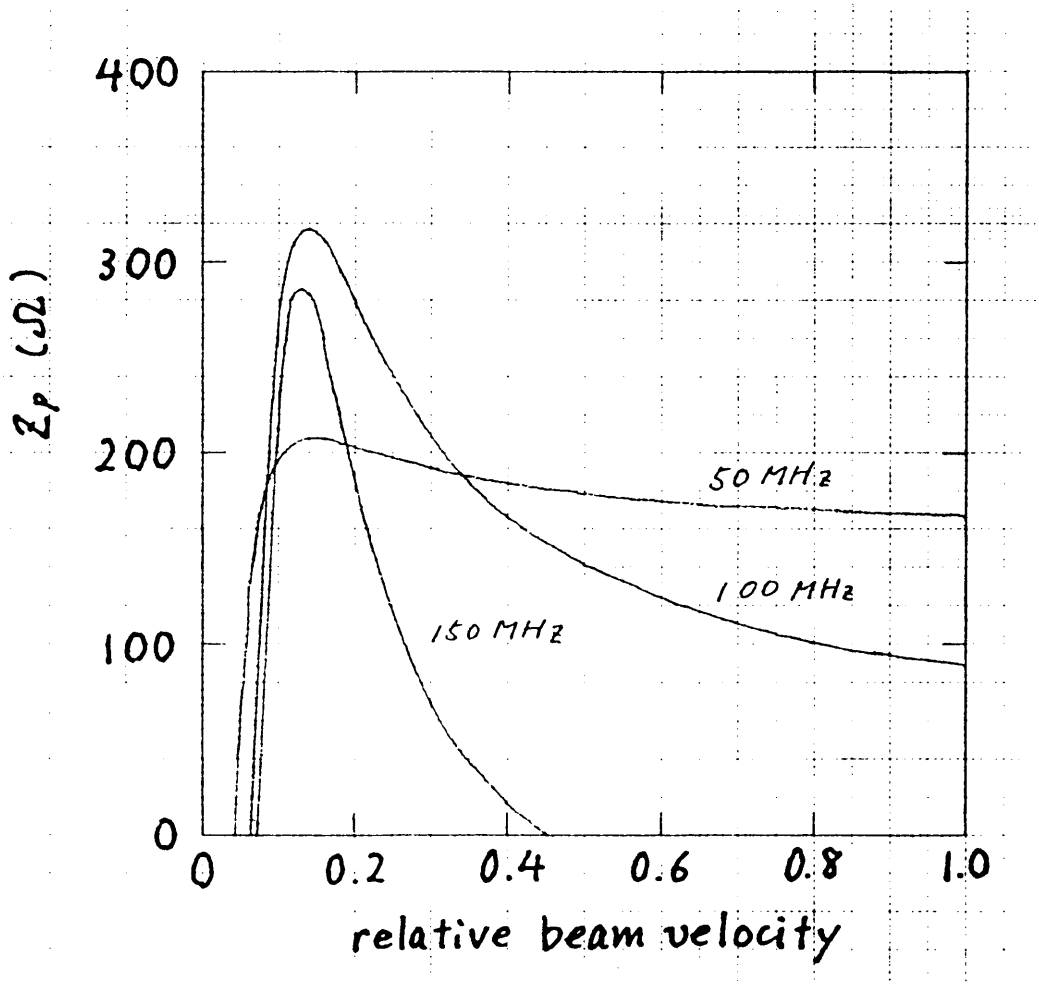

Fig. 13. Coupling impedances of the 36.2 cm − long coupler at 50, 100, and 150 MHz.

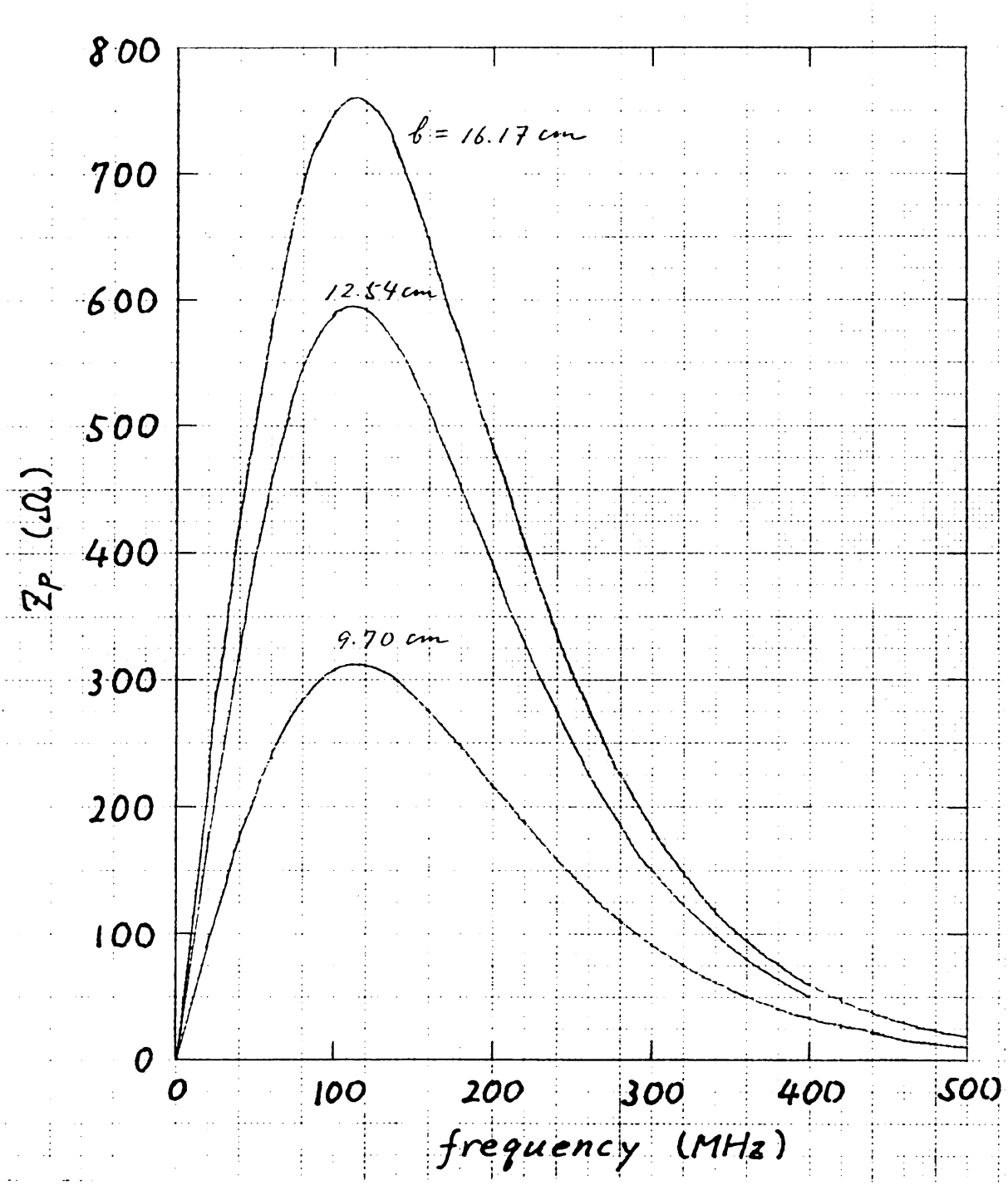

Fig. 14. Coupling impedance for some values of shield radius: 9.70 cm (b/a = 1.2), 12.54 cm (1.55), and 16.17 cm (2.0). The helix radius is 8.09 cm, the length is 72.4 cm, and $\sin\psi$ = 0.12147. The load resistances are equal to characteristic impedance at 0 MHz: 82 Ω for b = 9.70 cm, 177 Ω for 12.54 cm, and 253 Ω for 16.17 cm.

Distribution (open)

Groupe LEAR

D. ALLEN
E. ASSEO
E. BAECKERUD
S. BAIRD
J. BENGTSSON
M. CHANEL
J. CHEVALLIER
R. GALIANA
R. GIANNINI
F. IAZZOURENE
P. LEFEVRE
F. LENARDON
R. LEY
A. MACCAFERRI
D. MANGLUNKI
E. MARTENSSON
J.L. MARY
C. MAZELINE
D. MOEHL
G. MOLINARI
J.C. PERRIER
T. PETTERSSON
P. SMITH
N. TOKUDA
G. TRANQUILLE
H. VESTERGAARD

Distribution (of abstract)

PS Scientific Staff